Tangential Mass Addition for Shock/Boundary-Layer Interaction Control in Scramjet Inlets

M. E. White,* R. E. Lee,† M. W. Thompson,‡ and A. Carpenter§
Applied Physics Laboratory, Johns Hopkins University, Laurel, Maryland 20723
and
W. J. Yanta¶
Naval Surface Warfare Center, White Oak, Maryland 20903

A series of tests are being performed to investigate and characterize shock-wave/boundary-layer interactions typical of hypersonic inlets and to develop methods of controlling, through the use of tangential mass addition, regions of shock-induced separation. The major objectives are being accomplished in a multiphase experimental test program with complementary application of computational techniques. Presented herein are results from the proof-of-concept phase of testing. The feasibility of using Mach 3 tangential air injection to eliminate separation associated with the cowl-shock/innerbody boundary-layer interaction in a scramjet inlet model has been demonstrated. The experimental test program was complemented by a computational investigation that demonstrated the importance of mass addition injector location relative to the shock/boundary-layer interaction region.

Introduction

THE effect of shock-wave/boundary-layer interactions on the inlet performance of hypersonic air-breathing vehicles is of great importance. Inlet compression on typical hypersonic vehicles is accomplished with a very long external compression forebody followed by an inlet cowl that generates an internally reflective wave field. As a result, the highly viscous layer developed on the forebody and ingested into the inlet will be subject to strong adverse pressure gradients and may be prone to separation. The existing data base for such interactions is limited to relatively low Mach numbers and to geometries not typical of hypersonic inlets. It is the objective of this effort to perform a series of experiments to significantly extend the data base with which to characterize shock-wave/boundary-layer interactions typical of hypersonic inlets. A multiphase test program has been undertaken to characterize the onset and extent of shock-induced separations near expansion corners and to develop techniques for controlling the separation using tangential mass addition (TMA). Candidate injectant gases include air, steam, He, and H_2. Detailed surface and instream flow properties are being obtained to provide a data base for validation of computational fluid dynamics (CFD) codes. The results presented herein are from the proof-of-concept (POC) test phase of this program.

Presented as Paper 89-7086 at the AIAA 9th International Symposium on Air-Breathing Machines, Athens, Greece, Sept. 3-8, 1989; received Oct. 12, 1989; revision received April 12, 1990; accepted for publication April 19, 1990.

*Assistant Supervisor, Propulsion Group, Aeronautics Department. Member AIAA.
†Senior Staff Engineer, Propulsion Group, Aeronautics Department: Member AIAA.
‡Associate Staff Engineer, Propulsion Group, Aeronautics Department. Member AIAA.
§Assistant Data Analyst, Propulsion Group, Aeronautics Department.
¶Chief Technologist, Aerodynamics Branch (K24). Associate Fellow AIAA.

The model used in the POC test series was a planar scramjet inlet model consistent with the inward-turning scoop inlet concept.[1] Modifications to the inlet model included fabrication of two new throat blocks capable of tangentially injecting air at Mach 3 on the forebody ramp just upstream of the theoretical cowl-shock impingement point. Tests were conducted in the Naval Surface Warfare Center, White Oak, supersonic wind tunnel no. 2 at Mach numbers from 3.0 to 5.0.

An initial Mach 4 tunnel entry was conducted in which the ability to control shock-induced separation and the resulting unsteady inlet flowfield with the use of tangential mass addition was demonstrated. In a much more extensive test, entry data were obtained for Mach 3, 4, and 5 tunnel conditions with the model at zero angle of attack and for Mach 4 conditions with the model pitched to a 5 deg windward angle of attack essentially simulating conditions at the inlet cowl lip plane for Mach 3.5 tunnel conditions.

The effectiveness of tangential mass addition for control of the cowl-shock-induced boundary-layer separation was demonstrated at Mach 4 and 5. At the Mach 4, 5-deg angle-of-attack test condition the mass addition had only limited effectiveness. At Mach 3 the inlet flowfield was very unsteady, and mass addition was ineffective.

Previous Work

A significant amount of previous work has been done on the investigation and control of shock-wave/boundary-layer interactions over a wide range of conditions. A comprehensive review of such material is beyond the scope of this paper, but the reader is referred to two excellent review articles, one by Delery and Marvin[2] discussing work on shock-wave/boundary-layer interactions in general, and one by Delery[3] reviewing the state of the art in control of shock-wave/boundary-layer interactions. The most common technique for control of shock/boundary-layer interactions has been the use of boundary-layer bleed; however, the difficulties in ducting the bleed flow due to the extreme temperatures typical of hypersonic boundary layers and the large system volume requirements have resulted in the choice of boundary-layer energization with tangential mass addition as the principal controlling mechanism being investigated in this effort. Figure 1 shows some typical types of shock/boundary-layer interactions and a schematic representation of the use of tangential mass addition to energize the incoming boundary layer.

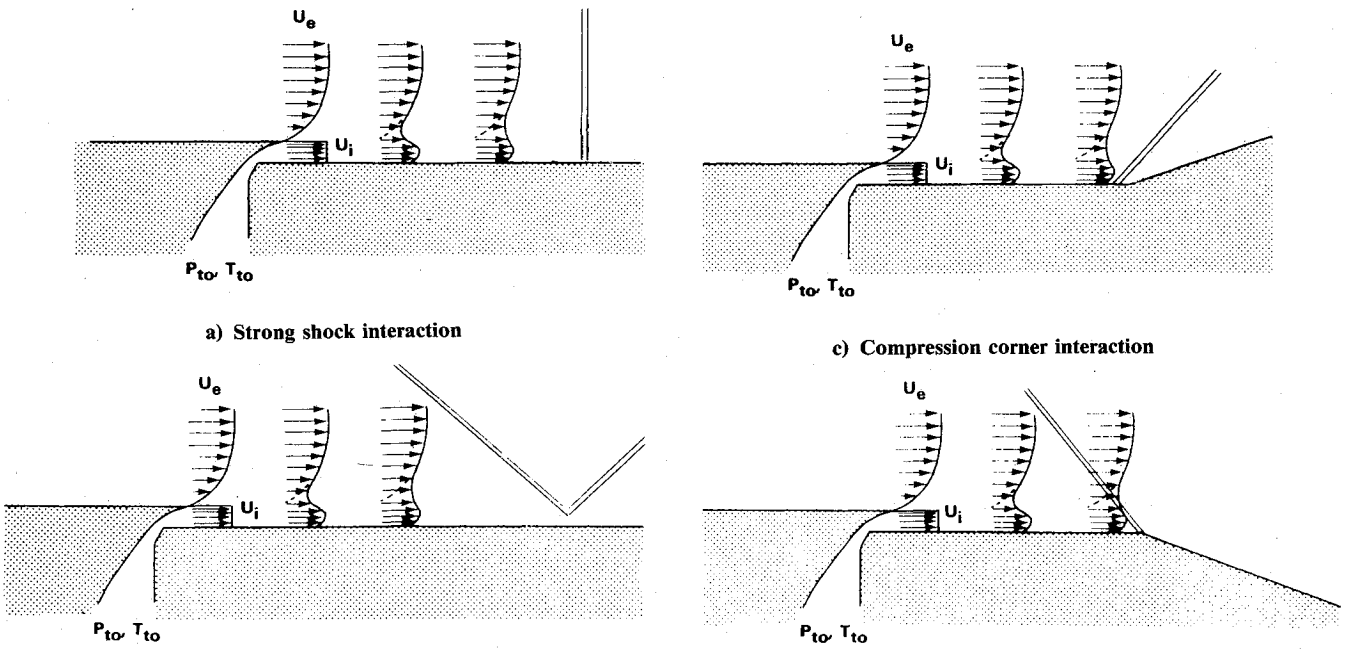

Fig. 1 Use of tangential mass addition to control various types of shock/boundary-layer interactions.

The strong-shock interaction shown in Fig. 1a is typical of the type of interaction that occurs when an external compression inlet is operating subcritically. Failure to control the interaction region in this instance can cause boundary-layer separation far upstream on the inlet ramp and often results in inlet "buzz." Work by Wong and Hall[4] and by Schwendemann[5] demonstrated the effective use of upstream mass addition for control of the strong-shock/boundary-layer interactions in a Mach 2 inlet.

The interaction of an incident oblique shock with a flat-plate boundary layer is shown in Fig. 1b. A significant amount of work has been done previously or is currently under way regarding this type of interaction. The main emphasis in that work has been to investigate the effect of the shock wave on wall film cooling effectiveness[6] or on shear layer growth.[7-9]

The use of tangential mass addition to control the shock/boundary-layer interaction at a supersonic compression corner, Fig. 1c, has received significant attention in past work by Grin[10] and Grin and Zakharov[11] in the Soviet Union and by several investigators[12-18] at the Indian Institute of Science.

The use of tangential mass addition to control the interaction of an incident shock with a boundary layer in the vicinity of an expansion corner, Fig. 1d, is typical of the phenomena of interest for hypersonic inlets and has received relatively little attention, an exception being the work by Ogorodnikov et al.[19] and Chernyy et al.[20] in the Soviet Union. It is this interaction in the vicinity of an expansion corner that is the main area of interest for the work being done under this effort.

Another type of shock/boundary-layer interaction noticeably lacking from the figures is the three-dimensional glancing shock interaction. These interactions occur in hypersonic inlets, either on the side walls due to shocks from forebody ramps and the cowl, or on the ramp and cowl if there exists a side-wall compression shock system. Peake[21] demonstrated that the use of slot injection along a line between the compression wedge angle and the resulting shock angle is effective for control of the three-dimensional glancing-shock interaction. Additional work on the use of tangential mass addition for control of shock/boundary-layer interactions has been published,[22-28] but, in general, the work has been done at low supersonic Mach numbers and for geometries not typical of hypersonic inlets.

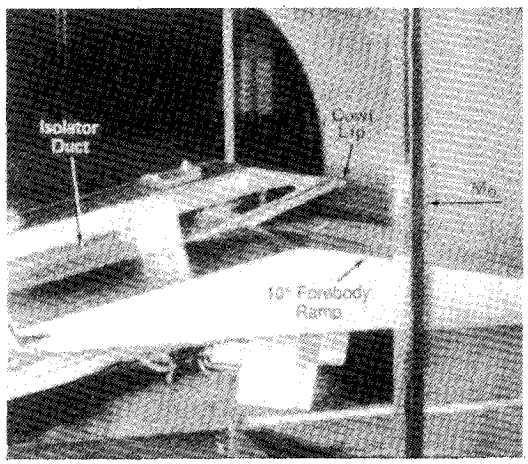

Fig. 2 Baseline proof-of-concept inlet model.

Discussion

Proof-of-Concept Inlet Model

POC test objectives were accomplished using a two-dimensional inward-turning scoop scramjet inlet model that consists of a 10-deg ramp followed by a cowl that turns the flow back along the inlet centerline (Fig. 2). The internal contour provides additional "isentropic" compression with both the cowl shock and the isentropic compression waves focused at a point inside the innerbody such that the inner surface becomes a streamline. The inlet is designed so that the forebody ramp shock falls on the cowl lip at a freestream Mach number (M_0) of 5 and the internal compression field is designed to be canceled by the innerbody contour upstream of the throat at a freestream Mach number of 3. The inlet model was equipped with transparent side walls to permit flow visualization of the internal flowfield.

Pitot and static pressure surveys were conducted at two stations downstream of the throat with access through model instrumentation ports located in the cowl surface. A pitot pressure survey was conducted on the inlet forebody ramp to characterize the incoming boundary layer at all test condi-

tions. Both external and internal flow visualization, accomplished using shadowgraph and oil flow, were recorded with video and 70-mm still photography. Real-time video monitoring of the inlet flow structure was accomplished using closed-circuit television.

The inlet model was modified to include Mach 3 tangential mass addition on the 10-deg innerbody ramp just upstream of the shoulder. The objective was to place the injection upstream of where the cowl shock/innerbody boundary-layer interaction takes place; however, the actual flexibility in placement of the nozzle was limited by the existing model geometry. Modification of the inlet model was accomplished by the fabrication of two new replaceable throat blocks, one of which is shown in Fig. 3, each with a nozzle that spans the 4-in. inlet duct. The nozzles have exit heights of 0.050 and 0.10 in., which are 5 and 10% of the baseline inlet throat height. The Mach 3 flow is achieved through a centered isentropic expansion. The nozzle was designed to be aligned with the forebody ramp, and the internal inlet contour downstream of the injection point was adjusted (opened by 0.050 or 0.10 in. as appropriate) to account for the injectant mass flow.

The throat blocks were easily interchangeable and were connected to a high-pressure air supply with regulation based on measured nozzle mass flow. Note the location of the static pressure taps on the block in Fig. 3. The seven centerline taps will be the first data points plotted on subsequent pressure distributions. In addition to the taps shown, centerline static pressures were measured on the innerbody at 1-in. increments throught the length of the isolator duct. A photograph of the 0.050-in. throat block installed in the POC inlet model, with the near inlet side wall removed, is shown in Fig. 4.

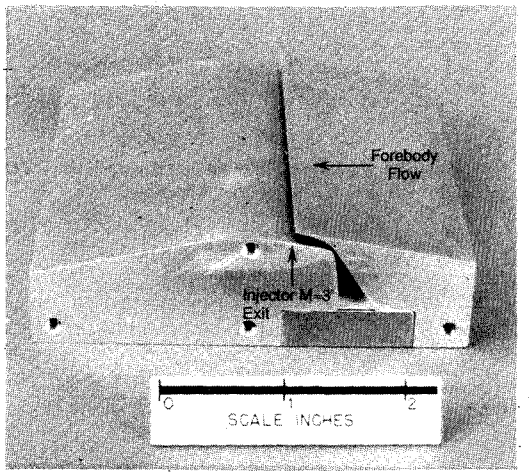

Fig. 3 Tangential mass addition throat block for the POC inlet model.

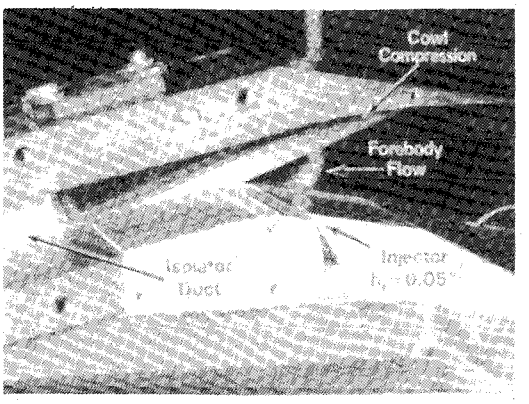

Fig. 4 H = 0.05 in. mass addition throat block installed in the POC inlet model.

It should be noted that there were no high response static pressure measurements made in this test entry. Therefore, pressure oscillations due to the unsteady inlet flowfields observed with no mass addition are not resolved in the data presented.

Wind-Tunnel Test Results

For the initial tunnel entry the inlet model was tested at Mach 4 using both the 0.050- and the 0.10-in. nozzles. During this test entry an experience base was gained on the operation of the inlet with various amounts of mass addition, and the injector nozzle flow was calibrated using a pitot survey in conjunction with wall static pressures. As evidenced from the shadowgraph pictures, it was determined that the cowl-shock-induced separation and resulting unsteady inlet flowfield that occurred for the baseline inlet could be controlled with both injector nozzles.

The second test entry included a 40-run test matrix at tunnel freestream Mach numbers of 3.0, 4.0, and 5.0 with the model at zero angle of attack (α). In addition, tests were conducted at Mach 4.0 with the model pitched to $\alpha = 5$ deg windward to simulate the cowl lip conditions for a $M = 3.5$, $\alpha = 0$ deg test condition. All tests were run with the tunnel in a continuous operating mode and for a supply total pressure and temperature of 1 atm and 560°R, respectively.

For all tests the tunnel flow was established with no mass addition, and the injection mass flow rate was gradually increased to its maximum level of 0.05 lbm/s. If the inlet separation was controlled, based on observation of either shadowgraph or oil flow video, then the controlling mass flow rate was noted and compared against the rate at which the separation reoccurred when the mass flow rate was decreased. In general, very little hysteresis was observed, and, in all cases, once the injectant mass flow was turned off the shock-induced separation and the resultant unsteady inlet flowfield reestablished.

Figure 5 shows a shadowgraph picture of the Mach 4 inlet flowfield with no mass addition. No appreciable shock structure is evident in the internal inlet duct, and a forebody separation and resulting shock are evident just below the swept-back side plate. Furthermore, this is a still photograph of a very unsteady inlet flowfield resulting from the shock-induced separation of the forebody boundary layer. Although oil flow gives only an indication of the near wall flow direction, some indication of the extent of the separated region can be seen in the oil flow photograph of Fig. 6.

The mass addition flow rate was gradually increased until the inlet flowfield, rather dramatically and suddenly, became very steady. The effectiveness of the mass addition in controlling the separation and creating a steady inlet flowfield is

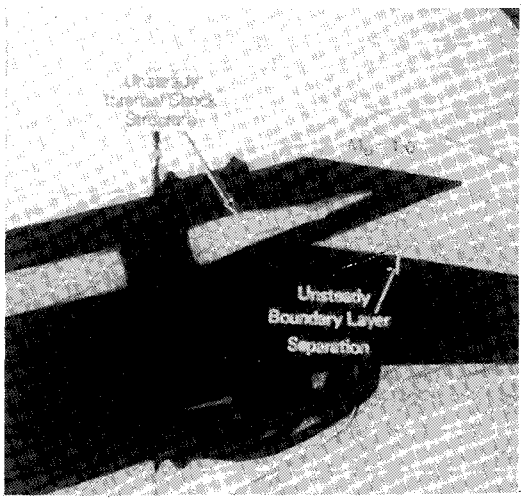

Fig. 5 Shadowgraph photograph of the Mach 4 inlet flowfield for the POC inlet model with no mass addition.

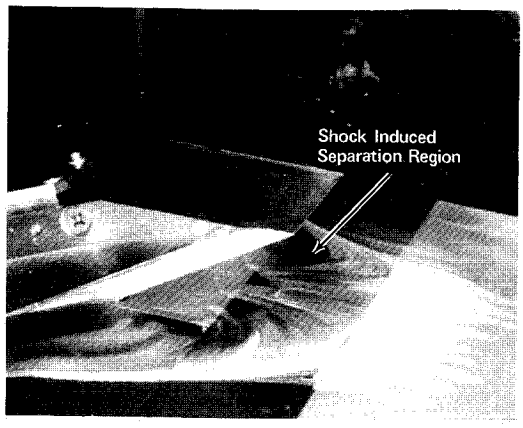

Fig. 6 Oil flow photograph of the Mach 4 inlet flowfield for the POC inlet model with no mass addition.

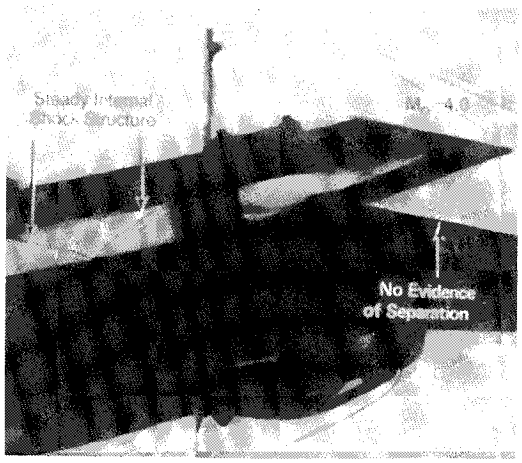

Fig. 7 Shadowgraph photograph of the Mach 4 inlet flowfield for the POC inlet model with mass addition.

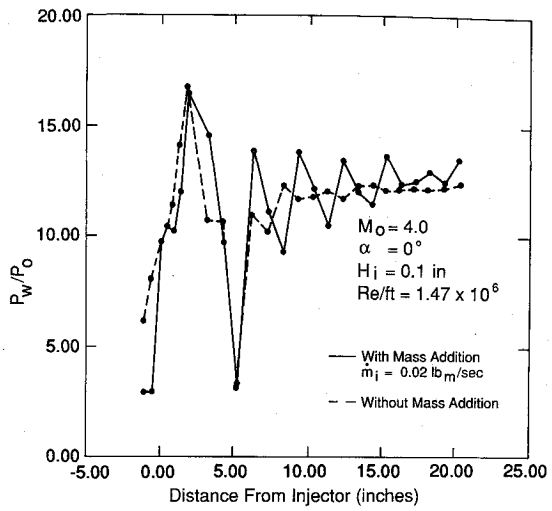

Fig. 8 Centerline static pressure distribution along the inlet innerbody at Mach 4 with and without mass addition.

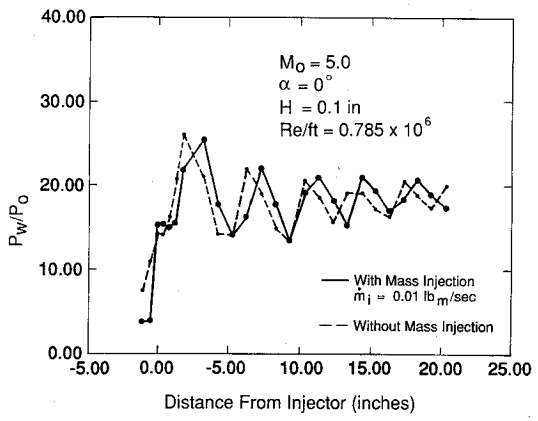

Fig. 9 Centerline static pressure distribution along the inlet innerbody at Mach 5 with and without mass addition.

shown in the shadowgraph photograph of Fig. 7. Clearly evident in the inlet "isolator" duct, the constant-area section downstream of the inlet throat designed to isolate the terminal shock system, is a well-defined shock structure, and there is no longer evidence of the forebody boundary-layer separation. Control of the inlet flowfield occurred at a mass flow rate of 0.017 and 0.022 lbm/s for the 0.05- and 0.10-in. injectors, respectively. The mass addition flow rates for control of the separation correspond to approximately 4 and 5%, respectively, of the captured inlet mass flow.

The centerline static pressure distribution along the inlet innerbody has been plotted in Fig. 8 at Mach 4 for the inlet configured both with and without mass addition. Again, the locations of the first seven data points are as shown in Fig. 3. Recall from the shadowgraph that the case with no mass addition showed a shock-induced boundary-layer separation upstream of the injector. The resulting shock from this separation is evident in the elevated static pressure. When mass addition was used at or beyond the controlling flow rate, elimination of the separated region is evidenced by the reduced static pressure level upstream of the injector. For this configuration the measured static pressure is equivalent to the expected static pressure for a 10-deg wedge at Mach 4. Also consistent with the shadowgraph, the shock system in the inlet isolator section is well defined, compared to the case with no mass addition, when the boundary-layer separation was eliminated.

A similar test sequence was performed at Mach 5. Again the inlet flowfield with no mass addition was very unsteady as a result of the forebody boundary-layer separation. The video and still shadowgraph pictures again showed evidence of the boundary-layer separation and the absence of a clearly defined inlet shock structure. Increasing the mass addition flow rate to a level of approximately 0.007 lbm/s (4–5% of the inlet captured mass flow) resulted in control of the separation and a very steady inlet flowfield with a well-defined inlet shock structure.

The centerline static pressure distributions at Mach 5, shown in Fig. 9, again indicate that the forebody pressure rise caused by the shock-induced separation is eliminated by use of tangential mass addition. For this case the separated region without mass addition was significantly smaller than it was at Mach 4. Although the video schlieren shows an unsteady inlet flowfield with no mass addition, the measured pressure distibution shows a distinct shock system in the isolator. Control of the separated region reduced the forebody pressure upstream of the injector and caused a slight shift in the inlet shock structure.

During the Mach 4 test series the mass addition flow rate was increased beyond the point at which the unsteady separation region was controlled while the model was at zero angle-of-attack. The model was then pitched 5 deg windward, and the inlet flowfield remained steady. The mass addition flow rate was gradually decreased until, at approximately the point at which the interaction was controlled at $\alpha = 0$ deg, the inlet flowfield became unsteady due to the cowl-shock/innerbody boundary-layer interaction. The mass addition flow rate was then increased to the maximum, and a steady inlet flowfield could not be re-established.

At Mach 3 test conditions the inlet flowfield was extremely unsteady with no mass addition. Increasing the mass addition flow rate to the limit of the supply system provided no control over the inlet flowfield.

The reason for the ineffectiveness of the mass addition at the lower Mach numbers was thought to be attributed to one of two factors. As the Mach number decreases, the cowl-generated shock becomes more steep and impinges on the forebody farther upstream. This results in the boundary-layer separation point being moved upstream relative to the injector location, thereby reducing the injector effectiveness. Also, the tunnel supply conditions were held constant at P_t = 15 psia and T_t = 560°R for all Mach numbers; therefore, the maximum available mass flow in the injector relative to the capture mass flow is reduced at the lower Mach numbers.

To identify mass addition ineffectiveness at the lower Mach numbers, computational flowfield solutions were generated in which the point of injection and the mass addition flow rates were varied for the low-Mach-number conditions. The results of this qualitative computational investigation are discussed in subsequent sections.

Computational Results

CFD flowfield solutions have been generated for the Mach 4 and 5 test conditions using a two-dimensional Navier-Stokes code, PARCH.[29] Because of the difficulties with the turbulence model in the vicinity of the mass addition nozzle, these calculations were run laminar downstream of the cowl lip; however, the inflow boundary-layer profiles were generated assuming turbulent flow up to the cowl lip. Flowfield convergence was based on mass conservation throughout the inlet.

Figure 10 shows the Mach 4 velocity vector diagram for the baseline inlet with no mass addition. The region of forebody boundary-layer separation is evident upstream of the inlet throat. The inlet geometry was modified to include the 0.10-in. injector geometry with a Mach 3 injector flow. Solutions were generated for several mass addition flow rates consistent with those tested in the experiment. When the injection rate was set at 0.01 lbm/s the separation, although reduced in size, was still evident. The injector mass flow was then set at 0.020 lbm/s and the forebody boundary-layer separation was completely eliminated as evidenced in the velocity vector diagram in Fig. 11. This compares favorably with the mass flow rate required to control the separation in the POC experiment, 0.022 lbm/s for the 0.10-in. injector.

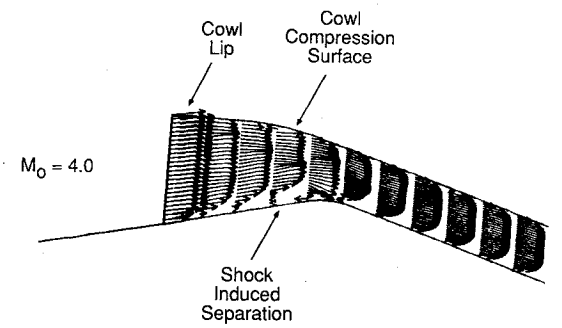

Fig. 10 Velocity vector diagram from a two-dimensional Navier-Stokes flowfield solution for the baseline POC inlet model at Mach 4.

For the Mach 5 flowfield solution of the baseline inlet with no mass addition, the extent of the separated region was less than that for the Mach 4 solution but still clearly evident in the velocity vector diagram. A computational solution for a mass addition flow rate of 0.01 lbm/s showed a complete elimination of the separated region. This again compared well with the experiment for which the boundary-layer separation was controlled at an injector mass flow rate of 0.007 lbm/s.

The results at Mach 4 and 5 provide sufficient confidence in the qualitative accuracy of the CFD solutions to permit use of the PARCH code for a numerical experiment to determine the effect of injector flow rate and injector location on the low-Mach-number effectiveness of tangential mass addition. In particular, CFD solutions were generated at the conditions for which the TMA was not effective in the test program to determine the effect of increasing the injector mass flow rate beyond the maximum tested and to determine the effect of moving the injection station upstream to the cowl lip.

A series of Navier Stokes solutions were run for the inlet model operating at Mach 3.5 and α = 0 deg, which is equivalent to the Mach 4, α = 5 deg condition tested for the baseline inlet model with no mass addition. For these conditions a stable converged inlet flowfield could not be obtained. Furthermore, investigation of the flowfield solution after several thousand interations indicated that the lack of convergence was due to inlet unstart and the fact that the upstream boundary conditions were ill-posed for subsonic inflow. The mass addition flow rate was set to 0.10 lbm/s, twice that achieved in the wind-tunnel tests, in the next attempt at a solution. Again, the inlet did not start, and a steady converged solution could not be obtained. A similar series of solutions were generated for Mach 3, α = 0 deg conditions. The velocity vector diagrams again indicated that, even with injection at a rate twice that achieved during the test, a stable and started inlet flowfield could not be achieved. These results seem to indicate that the maximum injection rate achievable during the experimental program was not the limiting factor in the inability to control the shock-induced separation and resulting unsteady inlet flowfield for the low-Mach-number test conditions.

A second numerical experiment was carried out to investigate the effect of injector location on the ability to control the shock/boundary-layer interaction. For this investigation

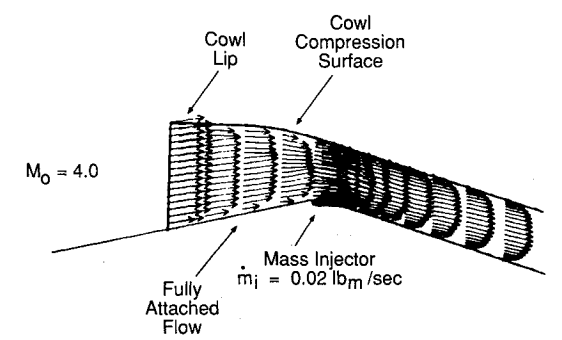

Fig. 11 Velocity vector diagram from a two-dimensional Navier-Stokes flowfield solution for the modified POC inlet model at Mach 4 with a mass addition flow rate of 0.02 lbm/s.

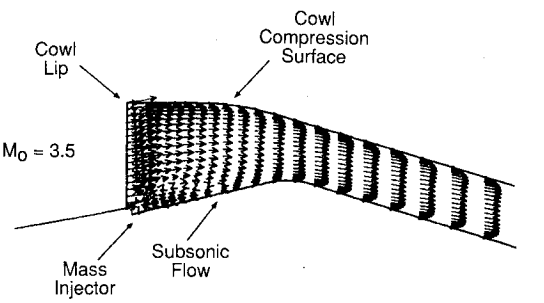

Fig. 12 Velocity vector diagram from a two-dimensional Navier-Stokes flowfield solution of the POC inlet model at Mach 3.5 with a forward injector but with no mass addition.

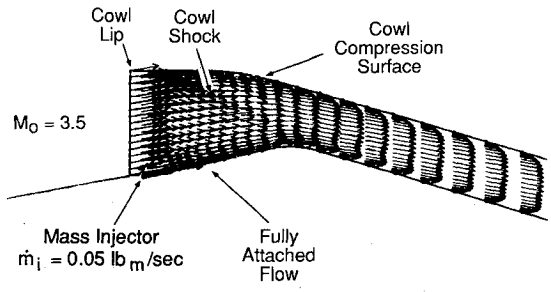

Fig. 13 Velocity vector diagram from a two-dimensional Navier-Stokes flowfield solution of the POC inlet model at Mach 3.5 with a forward injector at a mass addition flow rate of 0.05 lbm/s.

the injector was moved upstream to the cowl lip station. A Mach 3.5, $\alpha = 0$ deg solution was generated with no mass addition to determine if the additional internal area relief would allow the inlet to operate started. As indicated in the velocity vector diagram of Fig. 12, a steady converged solution for a started inlet could not be achieved. A solution was then generated with a mass addition flow rate of 0.05 lbm/s, consistent with the maximum injector flow rate run during the experiment and half of the maximum rate run computationally with the injector located downstream. As indicated in the velocity vector diagram of Fig. 13, the mass addition was sufficient to eliminate the shock-induced separation of the forebody boundary layer, allowing the inlet to start.

This demonstrates, within the accuracy of the computational tools applied, that the inability to re-establish control of the interaction region during the inlet tests at Mach 4, $\alpha = 5$ deg was due to the location of the injector relative to the interaction region. This highlights the criticality of placing the tangential mass addition upstream of the interaction region to energize the incoming boundary layer.

Similar solutions generated for Mach 3, $\alpha = 0$ deg conditions show that, even with the mass addition at the cowl lip and an injection rate as high as 0.10 lbm/s, the inlet did not start. Although the geometric internal contraction ratio of the baseline inlet is slightly below the theoretical starting limit, it seems that the mass addition was not sufficiently effective in controlling the forebody boundary-layer separation and prevent the resulting aerodynamic overcontraction.

Conclusions

The use of tangential mass addition as a boundary-layer energizing mechanism for control of shock/boundary-layer interactions occurring in scramjet inlets has been demonstrated for Mach numbers between 3.5 and 5.0. An experimental test program complemented by numerical investigations indicates that the position of the injector with respect to the boundary-layer separation point is an important factor in the effectiveness of the mass addition. Tests at Mach 4 and $\alpha = 5$ deg indicate that, at the position of the injector for this POC test, the mass addition was effective as long as the started inlet flowfield was established; however, once the boundary-layer separation was allowed to take place, the injector was not sufficiently far upstream to effectively re-establish control. At Mach 3.0, the inlet appears to be too close to the theoretical internal contraction starting limit to enable the mass addition to be effective even when placed as far upstream as the cowl lip.

Acknowledgments

This effort has been jointly sponsored at the National Aerospace Plane Joint Program Office by E. S. Gravlin and F. D. Stull and by Alan Roberts at the Office of Naval Research. Their support has been instrumental in allowing the successful execution of this program.

References

[1]Yanta, W. J., Collier, A. S., Spring, W. C., Boyd, C. F., and McArthur, J. C., "Experimental Measurements of the Flow in a Scramjet Inlet at Mach 4," AIAA Paper 88-271, Jan. 1988.

[2]Delery, J. M., and Marvin, J. G., "Shock-Wave Boundary Layer Interactions," AGARDograph No. 280, Feb. 1986.

[3]Delery, J. M., "Shock Wave/Turbulent Boundary Layer Interaction and its Control," *Progress in Aerospace Sciences*, Vol. 22, April 1985, pp. 209–280.

[4]Wong, W. F., and Hall, G. R., "Suppression of Strong Shock Boundary Layer Interaction in Supersonic Inlets by Boundary Layer Blowing," AIAA Paper 75-1209, Sept. 1975.

[5]Schwendemann, M. F., "Experimental Investigation of Tangential Blowing for Control of the Strong Shock Boundary Layer Interaction on Inlet Ramps," NASA CR-165390, June 1981.

[6]Goldstein, R. J., Eckert, E. R. G., Tsou, F. K., Haji-Sheikh, A., "Film Cooling with Air and Helium Injection Through a Rearward-Facing Slot into a Supersonic Air Flow," *AIAA Journal*, Vol. 4, June 1966, pp. 981–985.

[7]Visich, M., Jr., and Libby, P. A., "Experimental Investigation of Mixing of Mach Number 3.96 Stream in Presence of Wall," NASA TN-D247, Feb. 1960.

[8]Gilreath, H. E., and Schetz, J. A., "Transition and Mixing in the Shear Layer Produced by Tangential Injection in Supersonic Flow," ASME Paper 71-FE-24, Feb. 1971.

[9]Walker, D. A., Campbell, R. L., and Schetz, J. A., "Turbulence Measurements for Slot Injection in Supersonic Flow," AIAA Paper 88-0123, Jan. 1988.

[10]Grin, V. T., "Experimental Study of Boundary Layer Control by Blowing on a Flat Plate from $M = 2.5$," FTD-DT-23-611-68, Feb. 1969.

[11]Grin, V. T., and Zakharov, N. N., "Experimental Investigation of Effect of Tangential Blowing and Wall Cooling on Flow with Separation," *Fluid Dynamics*, Vol. 6, 1974, p. 1035.

[12]Viswanath, P. R., Sankaran, L., Sagdeo, P. M., Narisimha, R., and Prabhu, A., "Injection Slot Location for Boundary-Layer Control in Shock-Induced Separation," *Journal of Aircraft*, Vol. 20, Aug. 1983, pp. 726–732.

[13]Lakshmikantha, H., Vegnanarayan, H., and Srinivasan, G., "Effect of Fluid Injection on Shock Wave Boundary Layer Interaction," Dept. of Aerospace Engineering, Indian Institute of Science, Bangalore, Rept. 69-FM-7, Nov. 1969.

[14]Krishnamurthy, V., "Suppression of Shock Induced Separation Using Tangential Fluid Injection, Part I," Dept. of Aerospace Engineering, Indian Institute of Science, Bangalore, Mechanical Engineering Project Rept., 1973.

[15]Manjunath, A. R., "Suppression of Shock Induced Separation uisng Tangential Fluid Injection, Part II," Dept. of Aerospace Engineering, Indian Institute of Science, Bangalore, Mechanical Engineering Project Rept., 1973.

[16]Sagdeo, P. M., "Suppression of Shock induced Separation Using Tangential Fluid Injection, Part III," Dept. of Aerospace Engineering, Indian Institute of Science, Bangalore, Mechanical Engineering Project Rept., 1974.

[17]Sankaran, L., "Suppression of Shock Induced Separation Using Tangential Fluid Injection, Part IV," Dept. of Aerospace Engineering, Indian Institute of Science, Bangalore, Mechanical Engineering Project Rept., 1976.

[18]Prabhu, A., and Aswathanarayana, R. N. S., "Control of Shock-Induced Separation by Blowing: Boundary Layer Profiles," Dept. of Aerospace Engineering, Indian Institute of Science, Bangalore, Rept. 78FM5, 1978.

[19]Ogorodnikov, D. A., Grin′, V. T., and Zakharov, N. N., "Controlling the Boundary Layer in Hypersonic Air Intakes," First International Symposium on Air-Breathing Engines, Marseille, France, 1972.

[20]Chernyy, G. G., Levin, V. A., et al., "Theoretical and Experimental Study of the Motion of Gas in a Hypersonic Boundary Layer with Tangential Injection," FTD-ID(RS)T-1343-77, Aug. 1977.

[21]Peake, D. J., "Three-Dimensional Swept Shock/Turbulent Boundary-Layer Separations with Control by Air Injection," NRC-15579, July 1976.

[22]Peake, D. J., "The Use of Air Injection to Prevent Separation of the Turbulent Boundary Layer in Supersonic Flow," British Ministry of Aviation, Aeronautical Research Counsel CP-890 (67-21194), 1966.

[23]Howell, G. A., and Tatro, R. F., "Tangential Fluid Injection for

Control of Shock-Boundary Layer Interaction," AIAA Paper 66-656, June 1966.

[24]Gartshore, I. S., and Newman, B. G., "The Turbulent Wall Jet in an Arbitrary Pressure Gradient," *Aeronautical Quarterly*, Vol. 20, 1969, pp. 25–56.

[25]Hubbart, J. E., and Bangart, L. H., "The Turbulent Wall Jet with an Initial Boundary Layer," AIAA Paper 71-612, June 1971.

[26]Alzner, E., and Zakkay, V., "Turbulent Boundary-Layer Shock Interaction With and Without Injection," *AIAA Journal*, Vol. 9, Sept. 1971, pp. 1769–1776.

[27]Jones, J. W., Isaacson, L. K., and Vreeke, S., "A Turbulent Boundary Layer with Mass Addition, Combustion, and Pressure Gradients," *AIAA Journal*, Vol. 9, Sept. 1971, pp. 1762–1768.

[28]Cooper, J. R., and Korkegi, R. H., "Investigation of Self-Induced Blowing and Suction Across a Region of Shock Wave-Boundary Interaction (for a Turbulent Boundary Layer)," ARL-75-0181, June 1975.

[29]Sinha, N., York, B. J., and Dash, S. M., "Applications of a Generalized Implicit Navier-Stokes Code, PARCH, to Supersonic and Hypersonic Propulsive Flowfields," AIAA Paper 88-3278, July 1988.